Triple-Decker Complexes. 12.[1] Triple-Decker Complexes with Bridging Boratabenzene Ligands. Syntheses, Structures of $[(\mu\text{-}C_5H_5BMe)(FeCp^*)_2]PF_6$ and of $[(\mu\text{-}C_5H_5BMe)\{Rh(COD)\}_2]CF_3SO_3$, and Boratabenzene Transfer Reactions†

Gerhard E. Herberich,* Ulli Englert, Beate Ganter, and Christian Lamertz[3]

Institut für Anorganische Chemie, Technische Hochschule Aachen, D-52056 Aachen, Germany

Received July 2, 1996⊗

The orange complex $Cp^*Fe(C_5H_5BMe)$ (**1a**) was synthesized from $[Cp^*Fe(NCMe)_3]PF_6$ and $Li(C_5H_5BMe)$ in 91% yield. Electrophilic stacking reactions with metalloelectrophiles gave the triple-decker salts $[(\mu\text{-}C_5H_5BMe)(FeCp^*)_2]PF_6$ (**4**), $[(\mu\text{-}C_5H_5BMe)(FeCp^*)(RuCp^*)]CF_3SO_3$ (**5**), and $[(\mu\text{-}C_5H_5BMe)(FeCp^*)(MCp^*)](CF_3SO_3)_2$ with M = Rh (for **6**) and M = Ir (for **7**). Electrophilic stacking of $Rh(C_5H_5BMe)(COD)$ (**8**) with $[(COD)Rh(MeNO_2)_x]CF_3SO_3$ gave $[(\mu\text{-}C_5H_5BMe)\{Rh(COD)\}_2CF_3SO_3$ (**10**). The structures of the two triple-decker complexes **4** and **10** were determined by X-ray diffraction. Boratabenzene transfer reactions were found for the heterobimetallic salts **5**−**7**.

Introduction

Triple-decker complexes are known, inter alia, for many B−C ring systems with cyclic conjugation[4] and for the carbocyclic systems cyclopentadienyl[5] and benzene.[6] For a long time the boratabenzene ligand played the role of a missing link. Although a large variety of complexes are known where the boratabenzene ligand is monofacially coordinated to metals,[7−9] the bifacial coordination mode has only recently been observed, and up to now in only two species.[9]

The chemistry of triple-decker complexes with bridging cyclopentadienyl ligands is dominated by equilibria of types (1) and (2) with L_R = Cp. Syntheses of these complexes make use of the forward reaction, the electrophilic stacking reaction; the reverse reaction, the nucleophilic degradation, limits their stability. In the case of heterobimetallic triple-decker complexes (LM ≠ L′M′) there are two potential regiochemistries for the reverse reaction. Thus, equilibrium (2) comes into play and the combination of the two equilibria may result in a ring ligand transfer reaction. For instance, Cp-FeCp* (Cp = C_5H_5, Cp* = C_5Me_5) reacts with $[Cp^*Ir(OCMe_2)_3]^{2+}$ to give the triple-decker species $[Cp^*Fe(\mu\text{-}Cp)IrCp^*]^{2+}$, which slowly decays above 0 °C to give (inter alia) $[CpIrCp^*]^+$.[5c]

$$LML_R + [L'M'(solv)_3]^{n+} \rightleftharpoons [LM(\mu\text{-}L_R)M'L']^{n+} + 3solv \quad (1)$$

$$[L'M'L_R]^{(n-1)+} + [LM(solv)_3]^+ \rightleftharpoons [LM(\mu\text{-}L_R)M'L']^{n+} + 3solv \quad (2)$$

LM = Cp*Fe, Cp*Ru

L′M′ = Cp*Fe, Cp*Ru, Cp*Rh, Cp*Ir

solv = e.g. $MeNO_2$, Me_2CO, MeCN

A similar chemistry can be developed for analogous boratabenzene complexes. In this context we shall deal with sandwich compounds of type $\mathbf{1}^{n+}$, triple-decker cations of type $\mathbf{2}^{n+}$, and metalloelectrophiles of type $\mathbf{3}^{n+}$, all with Cp* ligands bound to the central metal. We shall also cover a related system with Rh(COD) fragments.

In an earlier paper we have already described the first two examples.[9] The ruthenocene analog $Cp^*Ru(C_5H_5BMe)$ (**1b**) readily undergoes an electrophilic stacking reaction with $[Cp^*Ru(OCMe_2)_3]^+$ (generated from $(Cp^*RuCl)_4$ and $AgCF_3SO_3$ in acetone) to form the triple-decker cation $[(\mu\text{-}C_5H_5BMe)(RuCp^*)_2]^+$ ($\mathbf{2e}^+$). Likewise, with $[Cp^*Rh(OCMe_2)_3]^{2+}$ the triple-decker cation [(μ-

† Dedicated to Professor Walter Siebert on the occasion of his 60th birthday.

⊗ Abstract published in *Advance ACS Abstracts,* November 1, 1996.

(1) Part 11: See ref 2.
(2) Herberich, G. E.; Jansen, U. J. *Organometallics* **1995**, *14*, 834.
(3) Lamertz, C. Doctoral Dissertation, Technische Hochschule Aachen, Aachen, Germany, 1996.
(4) Herberich, G. E. In *Comprehensive Organometallic Chemistry II*; Abel, E. W., Stone, F. G. A., Wilkinson, G., Eds.; Pergamon Press: New York, 1995; Vol. 1 (Housecroft, C. E., Volume Ed.), p 197.
(5) (a) Werner, H.; Salzer, A. *Synth. Inorg. Met.-Org. Chem.* **1972**, *2*, 239. Salzer, A.; Werner, H. *Synth. Inorg. Met.-Org. Chem.* **1972**, *2*, 249. Salzer, A.; Werner, H. *Angew. Chem., Int. Ed. Engl.* **1972**, *11*, 930. Dubler, E.; Textor, M.; Oswald, H. R.; Jameson, G. B. *Acta Crystallogr.* **1983**, *B39*, 607. (b) Kudinov, A. R.; Rybinskaya, M. I.; Struchkov, Yu. T.; Yanovskii, A. I.; Petrovskii, P. V. *J. Organomet. Chem.* **1987**, *336*, 187. Lumme, P. O.; Turpeinen, U.; Kudinov, A. R.; Rybinskaya, M. I. *Acta Crystallogr.* **1990**, *C46*, 1410. (c) Herberich, G. E.; Englert, U.; Marken, F.; Hofmann, P. *Organometallics* **1993**, *12*, 4039.
(6) (a) Duff, A. W.; Jonas, K.; Goddard, R.; Kraus, H.-J.; Krüger, C. *J. Am. Chem. Soc.* **1983**, *105*, 5479. Chesky, P. T.; Hall, M. B. *J. Am. Chem. Soc.* **1984**, *106*, 5186. Angermund, K.; Claus, K. H.; Goddard, R.; Krüger, C. *Angew. Chem., Int. Ed. Engl.* **1985**, *14*, 237. Jonas, K.; Rüsseler, W.; Angermund, K.; Krüger, C. *Angew. Chem., Int. Ed. Engl.* **1986**, *25*, 927. (b) Burdett, J. K.; Canadell, E. *Organometallics* **1985**, *4*, 805. Lamanna, W. M. *J. Am. Chem. Soc.* **1986**, *108*, 2096. Lamanna, W. M.; Gleason, W. B.; Britton, D. *Organometallics* **1987**, *6*, 1583.
(7) Herberich, G. E.; Ohst, H. *Adv. Organomet. Chem.* **1986**, *25*, 199.
(8) Bazan, G. C.; Rodriguez, G.; Ashe, A. J., III; Al-Ahmad, S.; Müller, C. *J. Am. Chem. Soc.* **1996**, *118*, 2291. Ashe, A. J., III; Kampf, J. W.; Müller, C.; Schneider, M. *Organometallics* **1996**, *15*, 387. Herberich, G. E.; Klein, W.; Spaniol, T. P. *Organometallics* **1993**, *12*, 2660.
(9) Herberich, G. E.; Englert, U.; Pubanz, D. *J. Organomet. Chem.* **1993**, *459*, 1.

S0276-7333(96)00536-5 CCC: $12.00

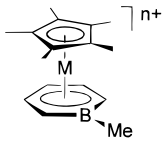

$[Cp^*M(C_5H_5BMe)]^{n+}$ (**1**)

1a: M = Fe, $n = 0$
1b: M = Ru, $n = 0$
1c$^+$: M = Rh, $n = 1$
1d$^+$: M = Ir, $n = 1$

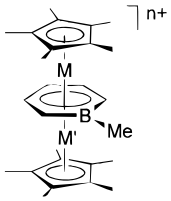

$[Cp^*M(\mu\text{-}C_5H_5BMe)M'Cp^*]^{n+}$ (**2**)

2a$^+$: M = Fe, M′ = Fe, $n = 1$
2b$^+$: M = Fe, M′ =Ru, $n = 1$
2c^{2+}: M = Fe, M′ = Rh, $n = 2$
2d^{2+}: M = Fe, M′ = Ir, $n = 2$
2e$^+$: M = Ru, M′ = Ru, $n = 1$
2f^{2+}: M = Ru, M′ = Rh, $n = 2$

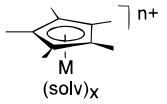

$[Cp^*M(solv)_x]^{n+}$ (**3**)

3a$^+$: M = Fe, $n = 1$
3b$^+$: M = Ru, n = 1
3c^{2+}: M = Rh, $n = 2$
3d^{2+}: M = Ir, $n = 2$

solv = $MeNO_2$, Me_2CO, MeCN

$C_5H_5BMe)(RuCp^*)(RhCp^*)]^{2+}$ (**2f**$^{2+}$) is formed, a solution species which slowly decomposes to produce $[Cp^*Rh(C_5H_5BMe)]^+$ (**1c**$^+$) and $[Cp^*Ru(OCMe_2)_3]^+$. Thus, the acetone solvent molecules effect a nucleophilic degradation of the dication **2f**$^{2+}$, which results in a boratabenzene transfer reaction.

In this paper we describe the syntheses of several more cationic triple-decker complexes with a bridging boratabenzene ligand. We also discuss some of their characteristic reaction chemistry.

Results and Discussion

Synthesis of $Cp^*Fe(C_5H_5BMe)$ (1a). The preparation of **1a**, like that of the ferrocene Cp^*FeCp, requires the stepwise addition of the two ligands to the iron center. The most obvious choice seemed to treat the Manriquez complex $[Cp^*Fe(acac)]_x$[10] with $Li(C_5H_5BMe)$.[11] Because of the lower nucleophilicity of the boratabenzene salt as compared to LiCp, the reaction mixture had to be warmed. As a consequence, dismutation products $FeCp^*_2$ and $Fe(C_5H_5BMe)_2$ formed, besides the desired product **1a**. Therefore, we turned to $[Cp^*Fe(NCMe)_3]PF_6$[12] as the source of the $FeCp^*$ fragment and found a fast and clean reaction with the lithium salt (Scheme 1). This gave a near-quantitative yield of **1a** as orange air-stable crystals. An X-ray structure determination confirmed the expected sandwich structure, with metal-to-ring distances of 165.8(5) pm for Fe−Cp* and 154.1(5) pm for Fe−(C_5H_5B).[13] The spectroscopic data of **1a** conform to expectation.

Scheme 1

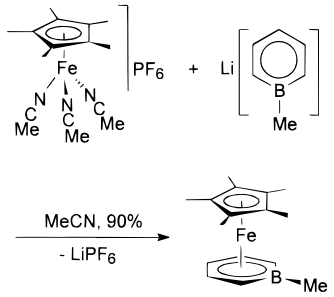

Syntheses of Triple-Decker Species. Complex **1a** readily undergoes electrophilic stacking reactions with metalloelectrophiles. When **1a** is treated with $[Cp^*Fe(NCMe)_3]PF_6$[12] or $[Cp^*Ru(NCMe)_3]CF_3SO_3$[14] in CD_2Cl_2 (NMR tube, 20 °C), a fast stacking reaction is observed. The intensely colored triple-decker cations, the purple cation **2a**$^+$ and the red cation **2b**$^+$, are formed quantitatively. During the subsequent removal of the CD_2Cl_2 under vacuum the cations suffer partial nucleophilic degradation as the acetonitrile concentration increases. This observation shows that the triple-decker formation is reversible. The product salts $[(\mu\text{-}C_5H_5BMe)(FeCp^*)_2]PF_6$ (**4**) and $[(\mu\text{-}C_5H_5BMe)(FeCp^*)(RuCp^*)]CF_3SO_3$ (**5**) can be precipitated from concentrated solutions by addition of a large volume of hexane.

The heterobimetallic cation **2b**$^+$ can also be obtained from the ruthenium sandwich complex **1b** and the iron electrophile $[Cp^*Fe(NCMe)_3PF_6$[12] (eq 4). The reversibility of the two coupled equilibria (3) and (4) implies transfer of boratabenzene ligands between the two metals involved.

$$\underset{\mathbf{1a}}{Cp^*Fe(C_5H_5BMe)} + \underset{\mathbf{3a,b}^+}{[Cp^*M(NCMe)_3]^+} \rightleftharpoons \underset{\mathbf{2a,b}^+}{[Cp^*Fe(C_5H_5BMe)MCp^*]^+} + 3MeCN \quad (3)$$

$$\underset{\mathbf{1b}}{Cp^*Ru(C_5H_5BMe)} + \underset{\mathbf{3a}^+}{[Cp^*Fe(NCMe)_3]^+} \rightleftharpoons \underset{\mathbf{2b}^+}{[Cp^*Fe(C_5H_5BMe)RuCp^*]^+} + 3MeCN \quad (4)$$

The isoelectronic and doubly charged triple-decker cations **2c**$^{2+}$ and **2d**$^{2+}$ are much more susceptible to nucleophilic degradation. It is therefore necessary to avoid all but the most non-nucleophilic species in the reaction system. The required metalloelectrophiles are

(10) Bunel, E. E.; Valle, L.; Manriquez, J. M. *Organometallics* **1985**, *4*, 1680.
(11) Herberich, G. E.; Schmidt, B.; Englert, U. *Organometallics* **1995**, *14*, 471.
(12) Catheline, D.; Astruc, D. *Organometallics* **1984**, *3*, 1094.
(13) In the solid state the molecules of **1c** showed a librational disorder in the C_5H_5BMe region and the bond distances were of poor quality within this ring (estimated standard deviations of up to 2 pm). For data and further details see ref 3.
(14) (a) $[Cp^*Ru(NCMe)_3]PF_6$: Schrenk, J. L.; McNair, A. M.; McCormick, F. B.; Mann, K. R. *Inorg. Chem.* **1986**, *25*, 3501. (b) $[Cp^*Ru(NCMe)_3]CF_3SO_3$: Fagan, P. J.; Ward, M. D.; Calabrese, J. C. *J. Am. Chem. Soc.* **1989**, *111*, 1698.

Table 1. ^{1}H NMR Spectral Data[a]

	4-H, 3-/5-H	2-/6-H	$^3J_{23}$	$^3J_{34}$	MCp*	FeCp*	BMe
1a	4.83	3.78	8.8			1.79	0.53
2a$^+$	5.03, 4.87	3.70	9.2	5.5		1.71	1.25
2b$^+$	4.90	3.81	7.9		1.83	1.70	0.99
2c^{2+}	6.25	5.06	8.2		1.98	1.85	1.15
2d^{2+}	6.17	4.94	7.9		2.07	1.85	1.25

[a] Recorded in CD_3NO_2 solution at 500 MHz and at ambient temperature; chemical shifts in ppm coupling constants in Hz.

produced from the chlorides $[Cp^*MCl_2]_2$ (M = Rh, Ir)[15] by dehalogenation with $AgCF_3SO_3$ in nitromethane.[16] The stacking reaction (5) with **1a** is smooth, and the

$$\underset{\mathbf{1a}}{Cp^*Fe(C_5H_5BMe)} + \underset{\mathbf{3a,b}^+}{[Cp^*M(MeNO_2)_x]^{2+}} \rightarrow \underset{\mathbf{2c,d}^{2+}}{[Cp^*Fe(C_5H_5BMe)MCp^*]^{2+}} + x MeNO_2 \quad (5)$$

product salts, the purple $[(\mu\text{-}C_5H_5BMe)(FeCp^*)(RhCp^*)]CF_3SO_3$ (**6**) and the red-brown $[(\mu\text{-}C_5H_5BMe)(FeCp^*)(IrCp^*)]CF_3SO_3$ (**7**), are isolated by removal of the solvent under vacuum or, in a higher state of purity, by crystallization from concentrated solutions at low temperature ($MeNO_2$, −30 °C).

The use of terminal Cp* ligands in the cations $\mathbf{2}^{n+}$ is convenient in several respects but not a necessity. To demonstrate this by a pertinent example, we treated $Rh(C_5H_5BMe)(COD)$[17] (**8**) in CH_2Cl_2 with a solution of $[(COD)Rh(solv)_x]CF_3SO_3$ (solv = CH_2Cl_2 or $MeNO_2$)[18] and obtained the orange product cation $\mathbf{9}^+$ via the stacking reaction (6). The cation $\mathbf{9}^+$ is extremely sensi-

$$\underset{\mathbf{4}}{Rh(C_5H_5BMe)(COD)} + [(COD)Rh(solv)_x]^+ \rightleftharpoons \underset{\mathbf{9}^+}{[(\mu\text{-}C_5H_5BMe)\{Rh(COD)\}_2]^+} + x\ solv \quad (6)$$

$$solv = CH_2Cl_2 \text{ or } MeNO_2$$

tive toward nucleophilic degradation, and the isolation of the product $[(\mu\text{-}C_5H_5BMe)\{Rh(COD)\}_2]CF_3SO_3$ (**10**) requires great care.

Characterization. The composition of the new compounds was established by elemental analyses and mass spectra. In the case of the particularly sensitive complex **10** a secondary ion mass spectrum could not be recorded.

The ^{1}H NMR data are collected in Table 1. Triple-decker formation is usually associated with a high-field shift for the central ring protons. For most proton signals of the triple-decker cations described here, the opposite is true, and the same has been noted previously for the corresponding triple-decker ions $[Cp^*Fe(\mu\text{-}Cp)MCp^*]^{n+}$ with bridging cyclopentadienyl rings (M and *n* as for **2a**,**b**$^+$ and **2c**,**d**$^{2+}$).[5c] The ^{11}B resonances of monofacially bonded 1-methylboratabenzene ligands lie in the range $\delta(^{11}B)$ 26.7−14.4;[7] for the new triple-decker ions they are shifted to higher field and range from δ 5.7 for **2b**$^+$ to δ 12.7 for **2c**$^{2+}$. The ^{13}C chemical shift data are collected in Table 2. A comparison with the data for the triple-decker ion **2e**$^+$ helped with the assignment, as did the quadrupolar line broadening of the signals for carbon atoms attached to a boron atom. The data are unexceptional.

Table 2. ^{13}C Chemical Shift Data[a]

	C-4	C-3/5	C-2/6[b]	MCp*	FeCp*	BMe[b]
1a	80.53	93.78	84.56		82.47, 10.20	2.02
2a$^+$	53.29	70.68	67.54		83.19, 9.75	−1.16
2b$^+$	54.08	70.47	68.74	89.44, 10.37	83.74, 9.91	−2.56
2c^{2+}	67.94	85.21	81.60	108.39,[c] 10.51	90.56, 9.62	−2.93
2d^{2+}	60.36	78.98	72.66	101.12, 9.99	90.78, 9.65	−3.66

[a] Recorded in CD_3NO_2 solution at 125.7 MHz and at ambient temperature; chemical shifts in ppm. [b] Signal with quadrupolar broadening. [c] $^1J(^{103}Rh-^{13}C)$ = 8.2 Hz.

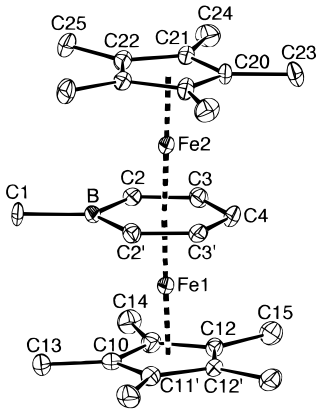

Figure 1. Thermal ellipsoid plot (PLATON)[20] of the cation **2a**$^+$ in compound **4**. Ellipsoids are scaled to 30% probability.

Table 3. Selected Bond Distances (pm) and Bond Angles (deg) for 4

(a) Distances

Fe1−B	223(1)	Fe2−B	222(1)
Fe1−C2	214.7(9)	Fe2−C2	215.0(9)
Fe1−C3	212.1(9)	Fe2−C3	211.7(9)
Fe1−C4	211(1)	Fe2−C4	212(1)
Fe1−C10	206(1)	Fe2−C20	203(1)
Fe1−C11	204.7(9)	Fe2−C21	205.3(9)
Fe1−C12	204.3(8)	Fe2−C22	204.3(8)
C2−B	152(1)	C1−B	161(2)
C2−C3	142(1)	C3−C4	143(1)

(b) Angles

C3−C2−B	122.5(9)	C2−B−C2′	113(1)
C2−C3−C4	121.4(9)	C1−B−C4	123.7(6)
C3−C4−C3′	120(1)		

The salts with the cations **2a**,**b**$^+$ and **2c**,**d**$^+$ show a strong CT band in the near-UV region and two broad d−d transitions in the visible region, which cause the colors of the triple-decker ions. The d−d bands are relatively intense, indicating considerable CT character.

Structure of 4. Purple crystals of **4** were obtained at −30 °C from a concentrated nitromethane solution and were characterized by X-ray crystallography (Table 3, Figure 1). The salt crystallizes in space group $P2_1/m$, and in agreement with packing considerations,[19] both cation and anion possess crystallographic mirror symmetry. The mirror plane contains Fe1, Fe2, C1, B, C4, and two C atoms of each Cp* ring as well as the atoms

(15) (a) Kang, J. W.; Moseley, K.; Maitlis, P. M. *J. Am. Chem. Soc.* **1969**, *91*, 5970. (b) Booth, B. L.; Haszeldine, R. N.; Hill, M. *J. Chem. Soc. A.* **1969**, 1299.
(16) Maitlis, P. M.; White, C.; Thompson, J. *J. Chem. Soc., Dalton Trans.* **1977**, 1654.
(17) Herberich, G. E.; Becker, H. J.; Carsten, K.; Engelke, C.; Koch, W. *Chem. Ber.* **1976**, *109*, 2382.
(18) Schrock, R. R.; Osborn, J. A. *J. Am. Chem. Soc.* **1971**, *93*, 3089.
(19) Brock, C. P.; Dunitz, J. D. *Chem. Mater.* **1994**, *6*, 1118.
(20) Spek, A. L. *Acta Crystallogr.* **1990**, *A46*, C34.

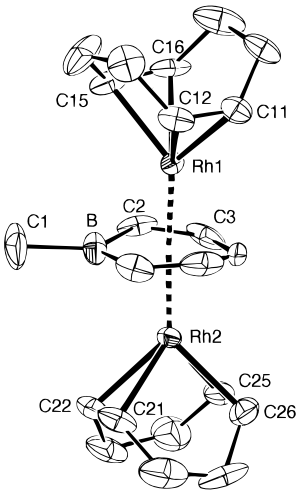

Figure 2. Thermal ellipsoid plot (PLATON)[20] of the cation $\mathbf{9}^+$ in compound **10**. Ellipsoids are scaled to 30% probability.

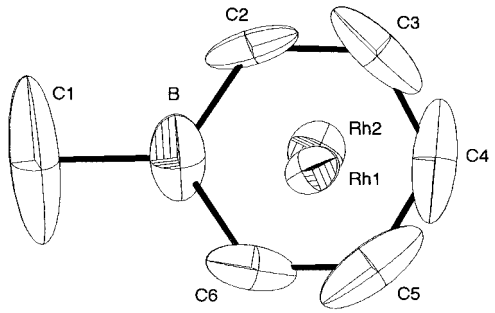

Figure 3. Central fragment of cation $\mathbf{9}^+$. Ellipsoids are scaled to 50% probability.

Table 4. Selected Bond Distances (pm) for 10

Rh1−B	239(2)	Rh2−B	238(2)
Rh1−C2	224(1)	Rh2−C2	243(2)
Rh1−C3	235(1)	Rh2−C3	227(1)
Rh1−C4	231(2)	Rh2−C4	223(1)
Rh1−C5	221(1)	Rh2−C5	233(2)
Rh1−C6	232(1)	Rh2−C6	227(1)
Rh1−C11	217(1)	Rh2−C21	212(1)
Rh1−C12	215(1)	Rh2−C22	216(1)
Rh1−C15	210(1)	Rh2−C25	215(1)
Rh1−C16	213(1)	Rh2−C26	214(1)
C2−B	150(2)	C6−B	148(2)
C1−B	160(2)		

P, F3, and F4. The observed orientation of the cation meets with our experience that the crystallographic mirror plane often contains the long axis of rod-shaped molecules. No intramolecular reasons would prevent an alternative arrangement with the boratabenzene ligand in the mirror plane.

The cation $\mathbf{2a}^+$ displays a typical triple-decker structure. The three rings are planar (largest vertical displacement 0.9 pm) and coplanar (with interplanar angles Cp*1,C_5H_5B = 2.7° and Cp*2,C_5H_5B = 1.0°); the metal-to-ring distances are 165.1(2) and 164.5(2) pm for the outer rings and 157.9(2) pm (twice) for the C_5H_5B ring. As expected, the bonds to the central ring are markedly longer than in the sandwich complex **1a**.

Structure of 10. A concentrated solution of **10** in CH_2Cl_2 was layered with hexane (8 volumes). Upon standing at ambient temperature orange needles formed that were suitable for X-ray crystallographic study (Table 4, Figures 2 and 3).

The overall picture of the cation $\mathbf{9}^+$ is that of a typical triple-decker species. However, the structure is also characterized by remarkably weak bonding between the rhodium and the boratabenzene ring. Thus, the metal-to-ring distances of 182.9 pm (av) for the C_5H_5B ring are surprisingly large, much larger than for the cation $\mathbf{2e}^+$, where the Ru−(C_5H_5B) distances average 174.2 pm (four observations for two independent molecules, minimum 173.7(1) pm, maximum 175.2(1) pm).[9]

Although the intensity data were collected at low temperature (203 K), rather large displacement parameters are found for the atoms of the CF_3 group and for the boratabenzene ring. Inspection of Figure 3 shows that the central ligand displays a librational motion around its center of gravity with the largest amplitudes at C1 and C4. Therefore, larger standard deviations of ca. 2 pm are associated with bond distances in the boratabenzene ligand of $\mathbf{9}^+$, despite the relatively good agreement factors.

Reactivity. The triple-decker salts of the cations $\mathbf{2a,b}^+$ and $\mathbf{2c,d}^{2+}$ are more stable than the corresponding triple-decker ions [Cp*Fe(μ-Cp)MCp*]$^{n+}$ with bridging cyclopentadienyl rings (M and *n* as for $\mathbf{2a,b}^+$ and $\mathbf{2c,d}^{2+}$).[5c] Nevertheless, nucleophilic degradation by solvent molecules is a very characteristic reaction of these salts. We report here a number of NMR tube experiments using the solvents nitromethane, acetone, and acetonitrile.

In nitromethane triple-decker formation is favored so much that the salt **4** does not show any signs of degradation over a period of 20 h, while **5** is stable for several days. However, in acetonitrile nucleophilic degradation takes place to a large extent. The species of equilibrium (3) are seen for **4** (92% **1a** after 24 h), while the slower degradation of **5** mainly gives **1b**, according to equilibrium (4) (14% **1a**, 38% **1b**, and 5% $\mathbf{2e}^+$ after 24 h). In acetone the reversible nucleophilic degradation is followed by a slower irreversible decomposition which produces the sandwich complex **1a** from **4** or **1b** from **5**, respectively. On prolonged reaction times insoluble material begins to appear and causes lines broadening in most of these experiments.

The dications $\mathbf{2c,d}^{2+}$ are much more susceptible to nucleophilic degradation because of the ensuing charge separation. When **6** is dissolved in acetonitrile the color changes from purple to orange; the products are complex **1a** and the acetonitrile-stabilized fragment [Cp*Rh(NCMe)$_3$]$^{2+}$.[16] The salt **7** reacts more slowly and is consumed completely within 1 week. We note that these reactions are irreversible and 100% regioselective.

Although the salts **6** and **7** can be made in nitromethane solutions according to (5), the solutions so obtained are not fully stable. On prolonged standing (1−10 days) signals of the new cations [Cp*M(C_5H_5BMe)]$^+$ (M = Rh, Ir)[21] ($\mathbf{1c,d}^+$) begin to appear. Thus, we observe a very slow and irreversible transfer of a boratabenzene ligand from Fe to Rh and Ir, respectively.

The sandwich complex **1a** and the cations $\mathbf{2a,b}^+$ are somewhat less easily oxidized than ferrocene. In CH_2Cl_2 they show chemically reversible oxidation reactions to give cations $\mathbf{1a}^+$ and $\mathbf{2a,b}^{2+}$, whereas $\mathbf{2e}^+$ shows a quasi-reversible oxidation at 1.23 V. The less stable cations $\mathbf{2c,d}^{2+}$ show irreversible oxidation reactions, both

(21) Cf. [Cp*M(C_5H_5BPh)]$^+$ with M = Rh, Ir: Herberich, G. E.; Engelke, C.; Pahlmann, W. *Chem. Ber.* **1979**, *112*, 607.

at 1.4 V in CH_2Cl_2, and irreversible reduction reactions at −0.51 (**2c**$^{2+}$) and −0.81 V (**2d**$^{2+}$) in THF at −20 °C. In the case of **2c**$^{2+}$ the reductive decomposition produces **1a** with its characteristic redox process at $E_{1/2} = 0.49$ V. Altogether, the only moderate stability of triple-decker complexes with bridging boratabenzene ligands is also limiting the number of accessible oxidation states.

Concluding Remarks. In this paper we have demonstrated that boratabenzene ions are able to act as bridging ligands in a variety of cationic triple-decker complexes. Generally these are more stable than the corresponding triple-decker complexes with bridging cyclopentadienyl ligands. On the other hand, they undergo nucleophilic degradation quite readily. In some cases triple-decker formation and nucleophilic degradation combine to effect a boratabenzene transfer reaction.

Experimental Section

General Procedures. Reactions were carried out under an atmosphere of dinitrogen by means of conventional Schlenk techniques. Solvents were purified and deoxygenated by conventional methods. Sand, Kieselguhr, and alumina (Woelm, N-Super O, activity I) were heated under high vacuum at 300 °C for 12 h and stored under dinitrogen; alumina was deactivated (5% H_2O, deoxygenated) after cooling. Florisil (Aldrich) was placed under high vacuum and flushed with dinitrogen several times prior to use. Melting points were measured in sealed capillaries and are uncorrected.

NMR spectra were recorded on a Varian Unity 500 spectrometer (^{1}H, 500 MHz; ^{13}C, 125.7 MHz; ^{11}B, 160.4 MHz), a Varian VXR 300 (^{1}H, 300 MHz; ^{13}C, 75.4 MHz), a Bruker WH-250 PFT (^{1}H, 250 MHz; ^{13}C, 62.9 MHz), a Bruker WP 80 PFT (^{1}H, 80 MHz), and a JEOL NM-PS-100 (^{11}B, 32.1 MHz); ^{1}H and ^{13}C spectra are referenced to internal TMS and ^{11}B spectra to external $BF_3{\cdot}OEt_2$. Mass spectra were recorded on a Varian MAT CH-5-DF (ionization by EI, 70 eV, nominal electron energy) and on a Finnigan MAT-95 spectrometer (for ionic compounds: SIMS from a DTT/DTE matrix).

Cyclic voltammetry was carried out using a EG&G 175 voltage scan generator and a EG&G 173 potentiostat. Solutions were ca. 10^{-3} M in electroactive species and 0.1 M in tetrabutylammonium hexafluorophosphate (TBAH) as supporting electrolyte. For the measurements a conventional three-electrode cell with a platinum-inlay working electrode, a platinum-sheet counter electrode, and a saturated calomel reference electrode (SCE) was used; the potential for the $FeCp_2^{+/0}$ couple was 0.38 V vs SCE in CH_2Cl_2 and 0.52 V vs SCE in THF. Abbreviations used in this text follow standard electrochemical conventions.[22] For example, E_p is the peak potential, v is the scan rate, and i_p is the peak current.

Preparation of 1a. A solution of [Cp*Fe(NCMe)$_3$]PF$_6$[12] (21.0 g, 45.7 mmol) in acetonitrile (120 mL) was added dropwise with stirring and cooling at 0 °C to a solution of Li(C$_5$H$_5$BMe)[12] (4.9 g, 50 mmol) in the same solvent (40 mL). The reaction mixture turned orange, and later crystals of **1a** formed. Stirring was continued for 1 h. The solvent was carefully removed under vacuum, and the residue was transferred to a frit which was covered by a layer (8 cm) of alumina. Extraction with hexane (500 mL) and removal of the eluent left **1a** (11.8 g, 91%) as orange crystals (mp 138 °C; sublimes at 90 °C/10^{-6} bar); the product can be recrystallized from EtOH. Anal. Calcd for $C_{16}H_{23}BFe$: C, 68.14; H, 8.22. Found: C, 68.07; H, 8.15. MS (EI): m/z (I_{rel}) 282 (100) [M$^+$]. ^{11}B NMR (C_6D_6): $\delta = 19$. CV ($v = 100$ mV s^{-1}, CH_2Cl_2, vs SCE): $E_{1/2} = 0.49$ V, $i_p^a/i_p^c = 1.02$.

Preparation of 4. A solution of [Cp*Fe(NCMe)$_3$]PF$_6$ (851 mg, 1.85 mmol) in CH_2Cl_2 (20 mL) was added to Cp*Fe(C$_5$H$_5$-BMe) (**1a**; 530 mg, 1.88 mmol) in CH_2Cl_2 (7 mL) at ambient temperature. After 1 h the deep purple reaction mixture was filtered through a frit covered with alumina (5% H_2O, 6 cm layer) and washed with CH_2Cl_2 until the eluate was colorless. The filtrate was concentrated to a small volume (10 mL) and layered with hexane (30 mL) to give **4** (740 mg, 65%) as purple crystals; dec >250 °C. Anal. Calcd for $C_{27}H_{38}BF_3Fe_2O_3S$: C, 50.52; H, 6.19. Found: C, 50.62; H, 6.08. SIMS (DTE/DTT matrix): m/z (I_{rel}) 473 (100) [**2a**$^+$], 326 (15) [FeCp*$_2^+$], 282 (10) [**1a**$^+$] for cations, 145 (100) [PF$_6^-$] for anions. ^{11}B NMR (CD_3NO_2): $\delta = 6.7$. Vis: λ/nm (ϵ_{max}/M^{-1} cm^{-1}) 410 (1530), 570 (950). CV ($v = 100$ mV s^{-1}, vs SCE): in CH_2Cl_2 $E_{1/2} = 0.65$ V, $i_p^a/i_p^c = 1.03$; in THF $E_{1/2} \approx -1.7$ V.

Preparation of 5. Solutions of **1a** (585 mg, 2.07 mmol) in CH_2Cl_2 (5 mL) and of [Cp*Ru(NCMe)$_3$]CF$_3$SO$_3$ (1.051 g, 2.07 mmol) in CH_2Cl_2 (8 mL) were combined and at kept at ambient temperature for 2 h. The solution immediately turned deep red. Workup as described for **4** using more hexane (80 mL) gave **5** (857 mg, 62%) as red crystals; mp 195 °C dec. Anal. Calcd for $C_{27}H_{38}BF_3FeO_3RuS$: C, 48.59; H, 5.74. Found: C, 48.41; H, 5.84. SIMS (DTE/DTT matrix): m/z (I_{rel}) 519 (100) [**2b**$^+$] for cations, 149 (100) [CF$_3$SO$_3^-$] for anions. ^{11}B NMR (CD_3NO_2): $\delta = 5.7$. Vis: λ/nm (ϵ_{max}/M^{-1} cm^{-1}) 410 (2660), 510 (1520). CV ($v = 100$ mV s^{-1}, vs SCE): in CH_2Cl_2 $E_{1/2} = 0.81$ V, $i_p^a/i_p^c = 1.09$; in THF $E_{1/2} \approx -1.8$ V.

Preparation of 6. $AgCF_3SO_3$ (1.03 g, 4.02 mmol) was added to a suspension of [Cp*RhCl$_2$]$_2$ (622 mg, 1.01 mmol) in nitromethane (8 mL), and this solution was stirred for 3 h at room temperature. Complex **1a** (558 mg, 1.98 mmol) was added, and stirring was continued for 1 h. The deep purple reaction mixture was filtered through Kieselguhr (2 cm). Removal of the solvent under vacuum gave **6** (1.42 g, 88%) as a purple solid; mp 211 °C dec. The product was then crystallized from highly concentrated solutions in $MeNO_2$ at −30 °C, collected on a frit, washed with a small amount of cold CH_2Cl_2, and dried under vacuum. Anal. Calcd for $C_{28}H_{38}BF_6FeO_6RhS_2$: C, 41.09; H, 4.68. Found: C, 41.10; H, 4.53. SIMS (DTE/DTT matrix): m/z (I_{rel}) 520 (55) [**2c**$^+$], 329 (100) [**3a**$^+$], 282 (35) [**1a**$^+$] for cations, 149 (100) [CF$_3$SO$_3^-$] for anions. ^{11}B NMR (CD_3NO_2): $\delta = 12.7$. Vis: λ/nm (ϵ_{max}/M^{-1} cm^{-1}) 500 (2450), 560 (1880). CV ($v = 100$ mV s^{-1}, vs SCE): in CH_2Cl_2 $E_{1/2} \approx 1.4$ V; in THF at −20 °C $E_{1/2} = -0.51$ V, $i_p^a/i_p^c = 0.84$.

Preparation of 7. Following the procedure described above for **6** with $AgCF_3SO_3$ (1.03 g, 4.02 mmol), [Cp*IrCl$_2$]$_2$ (803 mg, 1.01 mmol), and **1a** (569 mg, 2.02 mmol) gave **7** (1.63 g, 90%) as a red-brown crystalline solid; mp 207 °C dec. Anal. Calcd for $C_{28}H_{38}BF_6FeO_6IrS_2$: C, 37.05; H, 4.22. Found: C, 37.00; H, 4.08. SIMS (DTE/DTT matrix): m/z (I_{rel}) 609 (32) [**2d**$^+$], 419 (100) [**1d**$^+$], 282 (14) [**1a**$^+$] for cations, 149 (100) [CF$_3$SO$_3^-$] for anions. ^{11}B NMR (CD_3NO_2): δ 8.2. Vis: λ/nm (ϵ_{max}/M^{-1} cm^{-1}) 420 (1710), 510 (950). CV ($v = 100$ mV s^{-1}, vs SCE): in CH_2Cl_2 $E_{1/2} \approx 1.4$ V; in THF at −20 °C $E_{1/2} = -0.81$ V, with $i_p^a/i_p^c = 0.92$, 0.89, and 0.84 for scan rates of 200, 100, and 50 mV s^{-1}, respectively.

Redox data for [(μ-C$_5$H$_5$BMe)(RuCp*)$_2$]CF$_3$SO$_3$: CV ($v = 100$ mV s^{-1}, CH_2Cl_2, vs SCE): $E_{1/2} = 1.23$ V, $i_p^a/i_p^c = 1.20$.

Preparation of 10. $AgCF_3SO_3$ (335 mg, 1.30 mmol) was added to a suspension of [RhCl(COD)]$_2$ (320 mg, 0.65 mmol) in $MeNO_2$ (12 mL) and stirred for 2 h at ambient temperature. The reaction mixture was filtered through Kieselguhr (2 cm) into a solution of Rh(C$_5$H$_5$BMe)(COD)[17] (**8**; 382 mg, 1.27 mmol) (prepared from [RhCl(COD)]$_2$ and Li(C$_5$H$_5$BMe)[11] and sublimed twice) in CH_2Cl_2 (5 mL). The orange reaction mixture was stirred for 2 h. Then, the volatiles were removed under vacuum and the residue was dissolved in CH_2Cl_2 (10 mL). The product was precipitated with Et_2O, collected on a frit, washed with hexane, and dried under vacuum to give **10** (519 mg, 62%) as a light yellow powder; mp 124 °C dec. Layering a concentrated solution in CH_2Cl_2 with hexane (8 volumes) at room

(22) Bard, A. J.; Faulkner, L. R. *Electrochemical Methods, Fundamentals and Applications*; Wiley: New York, 1980.

Table 5. Crystallographic Data, Data Collection Parameters, and Refinement Parameters for 4 and 10

	4	**10**
formula	$C_{26}H_{38}BF_6Fe_2P$	$C_{23}H_{32}BF_3O_3Rh_2S$
fw	618.06	662.19
cryst syst	monoclinic	monoclinic
space group	$P2_1/m$ (No. 11)	$P2_1/n$ (No. 14)
a, pm	1006.3(5)	1439.3(4)
b, pm	1115.2(9)	1109.8(7)
c, pm	1276.9(4)	1574.2(7)
β, deg	106.80(3)	92.55(3)
V, nm^3	1.372(1)	2.512(3)
d_{calcd}, g cm^{-3}	1.498	1.751
Z	2	4
F(000)	640	1328
μ, cm^{-1}	95.93	14.17
cryst dimens, mm	0.32 × 0.8 × 0.10	0.3 × 0.1 × 0.04
radiation (λ, pm)	Cu Kα (154.18)	Mo Kα (71.073)
T, K	203	203
scan mode	ω	ω
scan range, deg	$5 \le \theta \le 70$	$3 \le \theta \le 25$
total no. of data	2616	7031
no. of unique obsd data	1506 ($I > \sigma(I)$)	2325 ($I > \sigma(I)$)
sec extinction coeff	0.768×10^{-6}	0.576×10^{-7}
no. of variables	182	299
R, R_w,[a] GOF	0.078, 0.071, 1.815	0.060, 0.041, 1.072
max resid density, 10^6 e pm^3	0.8 (140 pm from Fe1)	0.7 (in anion)

[a] Refinement on F; $R = \sum||F_o| - |F_c||/\sum|F_o|$; $R_w = [\sum w(|F_o| - |F_c|)^2/\sum w(F_o)^2]^{1/2}$; $w = 1/\sigma^2(F_o)$.

temperature gave large needles. Anal. Calcd for $C_{23}H_{32}BF_3O_3Rh_2S$: C, 41.72; H, 4.87. Found: C, 41.60; H, 4.66. ^{1}H NMR (500 MHz, CD_3NO_2): δ 6.06 (dd, 2H, 3-/5-H), 5.83 (t, 1H, 4-H), 4.96 (d, 2H, 2-/6-H), $^3J_{23} = 8.1$ Hz, $^3J_{34} = 5.2$ Hz, 4.71 (s, 8H, CH═), 2.31 (m, 8H, CH_2), 2.08 (m, 8H, CH_2), 0.78 (s, 3H, BMe). ^{11}B NMR (CD_3NO_2): δ 17.2.

X-ray Structure Determinations. Geometry and intensity data were collected on ENRAF-Nonius CAD4 diffractometers equipped with graphite monochromators. A summary of crystal data, data collection parameters, and convergence results is given in Table 5. Corrections for Lorentz−polarization, for absorption (empirical, by means of ψ scans),[23] and in the case of **4** for a slight linear radiation decay (less than 3% of the initial intensity) were applied. The structures were solved by direct methods (program SHELX-TREF)[24] and refined on structure factors.[25] Non-hydrogen atoms were refined anisotropically; hydrogen atoms were included in the refinement as riding atoms (C−H = 98 pm, $B_H = 1.3B_C$). In the final refinement, a correction for secondary extinction was applied to the calculated structure factors.[26,27]

Acknowledgment. We thank Hartmut Eckenrath for helpful discussions. This work was generously supported by the Deutsche Forschungsgemeinschaft and the Fonds der Chemischen Industrie.

Supporting Information Available: Tables of bond distances and angles, anisotropic thermal parameters, and atom coordinates for **4** and **10** (13 pages).[27] Ordering information is given on any masthead page.

OM960536M

(23) North, A. C. T.; Phillips, D. C.; Mathews, F. S. *Acta Crystallogr.* **1968**, *A24*, 351.
(24) Sheldrick, G. M. SHELXS-86, Program for Crystal Structure Solution; University of Göttingen, Göttingen, Germany, 1986.
(25) MolEN, An Interactive Structure Solution Procedure; ENRAF-Nonius, Delft, The Netherlands, 1990.
(26) Zachariasen, W. H. *Acta Crystallogr.* **1963**, *16*, 1139.
(27) Further details of the crystal structure analysis are available on request from the Fachinformationszentrum Karlsruhe, Gesellschaft für wissenschaftlich-technische Information mbH, D-76344 Eggenstein-Leopoldshafen, Germany, on quoting the depository numbers CSD-405875 for **4** and CSD-405876 for **10**, the names of the authors, and this journal citation.